

AFRL-SN-RS-TR-2002-255
Final Technical Report
September 2002



DYNAMICS OF TRIANGULAR AND SQUARE ARRAYS


Massachusetts Institute of Technology

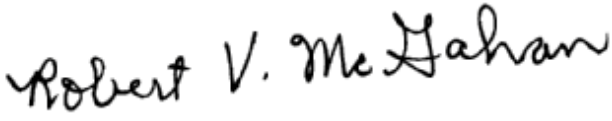
APPROVED FOR PUBLIC RELEASE; DISTRIBUTION UNLIMITED.

**AIR FORCE RESEARCH LABORATORY
SENSORS DIRECTORATE
ROME RESEARCH SITE
ROME, NEW YORK**

This report has been reviewed by the Air Force Research Laboratory, Information Directorate, Public Affairs Office (IFOIPA) and is releasable to the National Technical Information Service (NTIS). At NTIS it will be releasable to the general public, including foreign nations.

AFRL-SN-RS-TR-2002-255 has been reviewed and is approved for publication

APPROVED: 
STANFORD P. YUKON
Project Engineer

FOR THE DIRECTOR: 
ROBERT V. MCGAHAN, Technical Advisor
Electromagnetic Scattering Division
Sensors Directorate

REPORT DOCUMENTATION PAGE			Form Approved OMB No. 074-0188	
Public reporting burden for this collection of information is estimated to average 1 hour per response, including the time for reviewing instructions, searching existing data sources, gathering and maintaining the data needed, and completing and reviewing this collection of information. Send comments regarding this burden estimate or any other aspect of this collection of information, including suggestions for reducing this burden to Washington Headquarters Services, Directorate for Information Operations and Reports, 1215 Jefferson Davis Highway, Suite 1204, Arlington, VA 22202-4302, and to the Office of Management and Budget, Paperwork Reduction Project (0704-0188), Washington, DC 20503				
1. AGENCY USE ONLY (Leave blank)		2. REPORT DATE SEPTEMBER 2002		3. REPORT TYPE AND DATES COVERED Final Feb 96 – Feb 97
4. TITLE AND SUBTITLE DYNAMICS OF TRIANGULAR AND SQUARE ARRAYS			5. FUNDING NUMBERS C - F30602-96-1-0059 PE - 61102F PR - 2304 TA - BR WU - P1	
6. AUTHOR(S) Terry P. Orlando				
7. PERFORMING ORGANIZATION NAME(S) AND ADDRESS(ES) Massachusetts Institute of Technology Cambridge Massachusetts 02139			8. PERFORMING ORGANIZATION REPORT NUMBER N/A	
9. SPONSORING / MONITORING AGENCY NAME(S) AND ADDRESS(ES) Air Force Research Laboratory/SNHE 80 Scott Drive Hanscom AFB Massachusetts 01731-2909			10. SPONSORING / MONITORING AGENCY REPORT NUMBER AFRL-SN-RS-TR-2002-255	
11. SUPPLEMENTARY NOTES AFRL Project Engineer: Stanford P. Yukon/SNHE/ (781) 377-2968/ Stanford.Yukon@hanscom.af.mil				
12a. DISTRIBUTION / AVAILABILITY STATEMENT APPROVED FOR PUBLIC RELEASE; DISTRIBUTION UNLIMITED.				12b. DISTRIBUTION CODE
13. ABSTRACT (Maximum 200 Words) The DC characteristics of single triangular Josephson Junction (JJ) cells and single row arrays have been studied to their potential as rf oscillators. Measurements of under damped systems reveal two steps in the current voltage (IV) characteristic, corresponding to LSC and LJ resonances. These steps are characteristics of single cells, and their position does not change significantly with array size. Measurements of two different cell sizes showed that the upper step voltage depends strongly on the cell geometry, while the lower step is only slightly affected. At the LSC resonance, underdamped arrays produce large amplitude single harmonic oscillations in the horizontal junctions. According to DC measurements oscillators based on this resonance operate at frequencies ranging from 70 - 170 GHz, with bandwidths of 10% - 20%. For 9mm ² junctions, the power expected from M horizontal junctions is M ² nW for low current densities and M ² lnW for high current densities. To study the possibility of mode locking in a 2D triangular array, simple diamond cells have been investigated. In addition to a common bias current, a small trim current applied to the bottom triangle of a diamond will engender an rf voltage at two frequencies corresponding to the upper and lower cell oscillations. The DC properties of the diamond system have been confirmed, and on chip measurements of the system are planned to confirm the response of the horizontal junction to trim current tuning.				
14. SUBJECT TERMS Josephson, Junction, Array, Oscillator, Mode Locked Pulse				15. NUMBER OF PAGES 11
				16. PRICE CODE
17. SECURITY CLASSIFICATION OF REPORT UNCLASSIFIED	18. SECURITY CLASSIFICATION OF THIS PAGE UNCLASSIFIED	19. SECURITY CLASSIFICATION OF ABSTRACT UNCLASSIFIED	20. LIMITATION OF ABSTRACT UL	

Table of Contents

1. Executive Summary	1
2. Research Progress	2
References	7

List of Figures

Figure 1: Current Voltage characteristics of single triangular cell and of an 8-cell array	3
Figure 2: Step voltage vs. field is compared to critical current vs. field for the 8-cell triangular array.	4
Figure 3: Current-voltage characteristics compared for a high current density	4
Figure 4: Diamond Cell	6

List of Tables

Table 1: Triangular Array Parameters	4
--------------------------------------	---

1 Executive Summary

The progress on the following tasks is as follows:

1.1.1 Design of triangular and one-dimensional arrays. Two new sets of designs were done in collaboration with S. Yukon, L. Caputo, and A. Utinov. These designs were submitted in September and October of 1996 to Hypres, Inc.

1.1.2 Fabrication of the arrays. Both sets of designs have been fabricated, and one has been measured.

1.2.1 Feasibility study of on-chip microwave sensors. The first round of such sensors have been measured. Based on these results, a new sensor has been designed and fabricated.

1.2.2 Feasibility study of direct microwave measurements. A. Duwel has visited Rome laboratories and learned the types of facilities available in the laboratories used by

J. Derov and J. Habib. A 10 GHz probe compatible with this equipment is in the process of being built. In addition, A. Duwel has worked with L. Caputo and A. Ustinov at KFA in Juelich, Germany, to design circuits which will be measured in the W-band at KFA. The facilities for these measurements are available at KFA and the testing will be completed by L. Caputo.

2 Research Progress

2.0.1 Samples and Parameters

We use samples made at HYPRES, with Nb-AlO_x-Nb junctions. HYPRES offers a minimum junction size of $9\mu\text{m}^2$ and critical current densities of 1000 kA/cm^2 and 100 kA/cm^2 . The capacitance of these junctions is approximately $C = 340\text{ fF}$. The normal-state resistance will be approximately $1.9\text{ mV}/I_c$. Thus, for high current density samples, $I_c = 90\mu\text{A}$ and $R_n = 21\Omega$. For low current density samples, $I_c = 9\mu\text{A}$ and $R_n = 211\Omega$. In practice, we measure the normal-state resistance to determine the junction critical current. Past studies have shown less than 5% variation in junction critical currents across a chip.

Our measurements are made in a ^4He probe. We use a μ -metal foil inside the

vacuum can for rf shielding. A solenoid surrounding the sample carrier allows the application of magnetic fields perpendicular to the sample plane up to 300 mG. A resistor attached to the sample carrier enables us to stabilize temperatures from 4.2 – 12 K.

Two main parameters, which can both be influenced by temperature, characterize our systems. The discreteness parameter, $\Lambda_J = L_J/L_s$, relates to the spatial extent of vortices in an array. It is given by the ratio of the junction inductance, $L_J = \Phi_o/(2\pi I_c)$, to the geometric inductance of a single cell, L_s . The Stewart-McCumber parameter $\beta_c = R_J^2 C/L_J$ defines the amount of damping in a single junction. We often use the junction normal-state resistance for R_J . For given values of critical current density, junction size, and cell size, the values of Λ_J and β_c are determined at 4.2 K. By raising the temperature, Λ_J^2 can be increased by a factor of 4 and β can be decreased by 75%.

We have designed arrays for four different parameter regimes, determined by the possible combinations of low current density, high current density, and the presence or absence of a shunt resistor. In addition, the size of the cell influences the parameter range. Table 2 summarizes the possibilities. We have included the minimum and maximum cell sizes which have been designed, although the smaller shunted cells have

not yet been measured. Ranges are listed for β and Λ_J^2 , consistent with changes in temperature.

2.0.2 Triangular Arrays as Local Oscillators

In order to determine the potential for triangular arrays as oscillators, we begin by studying the dc characteristics of single cells and single row arrays.

Measurements of underdamped systems reveal two steps in the current-voltage (IV) characteristic, corresponding to $L_s C$ and $L_J C$ resonances [1, 3]. These steps are characteristics of single cells, and their position does not change significantly with array size. Measurements of two different cell sizes showed that the upper step voltage depends strongly on the cell geometry, while the lower step is only slightly affected. In Figure 1, we compare the IV of a triangular cell with parameters $\beta = 230$ and $\Lambda_J^2 = 2.4$ to that of a 9-cell array with the same parameters. The steps appear only in the presence of a magnetic field, when the average applied flux per cell (called frustration, f) is approximately one-half. They are stable for a range of $f = 0.3 - 0.7$. Figure 2 shows the range of stability and the step voltage variation, by plotting the step voltage together with the array critical current vs. frustration. Both are periodic in field. As usual, the critical current is largest at $f = 0$, while the steps maxi-

mize at $f = 0.5$.

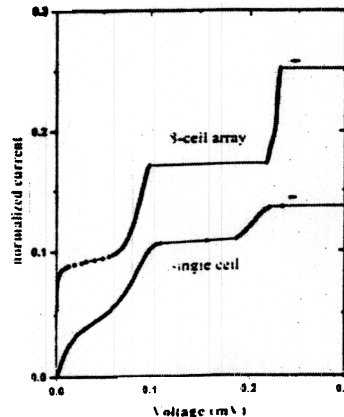


Figure 1: Current-Voltage characteristics of a single triangular cell and of an 8-cell array. The parameters are $\beta = 230$ and $\Lambda_J^2 = 2.4$, and $f = 0.5$.

These steps also appeared in measurements of high critical current density junctions, where the devices more damped ($\beta \sim 10$) and more discrete ($\Lambda_J^2 \sim 0.6$). At low temperatures, these samples have Λ_J^2 values well below 1. We found that the upper step, corresponding the $L_s C$ resonance, is only stable when the temperature is raised such that $\Lambda_J^2 > 0.3$ (approximately). We observed, unexpectedly, that *both* step voltages showed a dependence on L_J through the critical current density. For identical geometric designs, low current density devices (discussed above) produce resonances at 0.1 and 0.23 mV, while the corre-

Table 1: TRIANGULAR ARRAY PARAMETERS

I_c	R_J	L_J	A_{min}, A_{max}	$L_s(min), L_s(max)$	$\Lambda_J^2(min), \Lambda_J^2(max)$	β
9 μA	211 Ω	36 pH	72.5, 252 μm^2	11, 20 pH	3.3 – 13, 1.8 – 7	422 – 105
90 μA	21 Ω	3.6 pH	72.5, 252 μm^2	11, 20 pH	0.3 – 1.3, 0.18 – 0.72	42 – 10
9 μA	1 Ω	36 pH	266, 1105 μm^2	20, 42 pH	1.8 – 7.2, 0.85 – 3.4	0.01 – 0.002
90 μA	1 Ω	36 pH	266, 1105 μm^2	20, 42 pH	0.18 – 0.72, 0.08 – 0.34	0.1 – 0.02

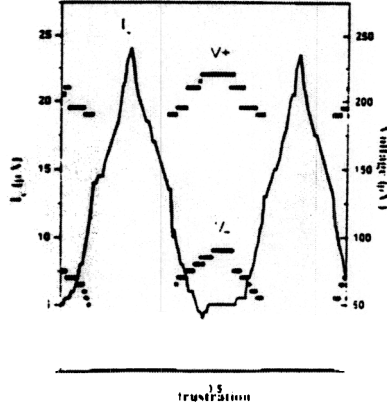


Figure 2: Step voltage vs. field is compared to critical current vs. field for the 8-cell triangular array.

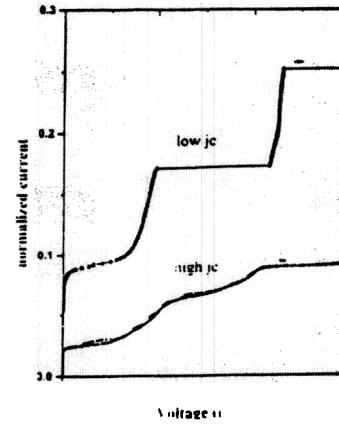


Figure 3: Current-voltage characteristics compared for a high current density ($j_c = 1000 \text{ kA/cm}^2$) and a low current density ($j_c = 100 \text{ kA/cm}^2$) 8-cell triangular array. The low j_c array has $\beta = 230$ and $\Lambda_J^2 = 2.4$, and the high j_c array has $\beta = 6.5$ and $\Lambda_J^2 = 0.6$.

sponding steps in high current density devices occurred at 0.12 and 0.20 mV respectively. Current-voltage characteristics for a low current density and a high current density sample are compared in Figure 3. Apparently, the upper step is more complicated than an L, C resonance, and a higher-order dependence on L_J should be included.

For overdamped junctions, we used

shunt resistors of approximately 1Ω . In both low current density and high current density samples, this dominates the shunt resistance. Including the shunt resistors made the cell size much larger. Thus the shunted systems are all highly discrete, and we do not expect the L,C resonance to be stable. Typical IV's show critical currents, but no other obvious nonlinearities. Lock-in measurements of the resistance reveal a slight nonlinearity. At this point, we have not definitively connected its voltage position with any particular resonance.

At the L,C resonance, underdamped arrays produce large-amplitude single-harmonic oscillations in the horizontal junctions [1]. According to dc measurements, oscillators based on this resonance operate at frequencies ranging from 70 – 170GHz, with bandwidths of 10 – 20%. For $9\mu\text{m}^2$ junctions, the power expected from M horizontal junctions is $M \times 2\text{ nW}$ for low current densities and $M \times 21\text{ nW}$ for high current densities. In our overdamped arrays, we have not yet identified an L,C resonance in the IV characteristic.

With W-band measurements, the output frequency, power, and linewidth can be confirmed. In collaboration with P. Caputo and A. Ustinov at KFA, two triangular rows have been coupled to fin-line antennas. A stripline with characteristic impedance approximately equal to the expected L,C res-

onance couples the horizontal junctions to the antenna. The fin-line antenna acts as a matched transition to the 80 – 120 GHz rectangular waveguide. Measurements will be made using facilities available at KFA by P. Caputo.

On-chip measurements can also be used to determine the output frequency and power. We plan to couple the output of triangular row oscillators to detector junctions. With good coupling, many researchers have found this to be an effective measurement technique. Radiation emitted from the oscillator excites Shapiro steps in the detector junction. Using simulations of the detector junction, the oscillator frequency and power can be inferred. We plan to use this method to compare the output of triangular rows with various lengths. Power measurements of these systems will allow us to determine the degree of phase-locking. We will measure the dependence of output power on frequency, using a magnetic field to tune the oscillator.

2.0.3 Mode-locking in 2D Triangular Arrays

To study the possibility of mode-locking in a 2D triangular array, we first investigated simple diamond cells, as shown in Figure 4. When a single bias current is applied to the vertical junctions, both the top triangular cell and the bottom cell have the same dc

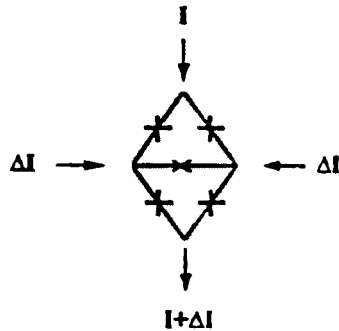


Figure 4: Diamond Cell

voltage. Next a small trim current, ΔI , is applied at the edges and removed at the same ground as the bias current. Thus more current is effectively passed through the lower cell. This causes the voltage across the lower junctions to increase relative to the upper cell junctions. On the oscilloscope, the entire IV of the lower cell is translated in voltage as the trim current is applied. Although no dc voltage develops across the horizontal junction, it develops a sinusoidal ac voltage at a two frequencies, corresponding to the upper and lower cell oscillations [2]. So far, we have confirmed the dc properties of this system. We intend to use on-chip measurements to confirm the response of the horizontal junction to tuning.

We have designed two row arrays, with tuning currents similar to the dia-

mond discussed above. We will check that the tuning is still effective in longer systems. Finally, we will measure multi-row systems. We have designed five row arrays with leads at the edges for the application of trim currents. It is important to apply equal trim currents into the array edges and remove them at the bottom. At the same time, we would like to use a single source for the trim currents. These conditions make the array design challenging. We have made two identical five-row arrays with different configurations for the trim currents. Our goal is to bias the five rows with incrementally increasing dc voltages. We will test the range of voltages that can be achieved and the effect of magnetic field on this state.

Once the array properties have been established through dc measurements, we will address the task of testing the high frequency properties. Our first step will be to make on-chip measurements of single rows which are part of a larger array. We will compare this data with data taken from isolated rows of equal length. Thus, we will measure the effect of the array on the output of a single row. Our next task will be to couple the outputs of two or more rows to a detector junction. We will bias the rows to oscillate at the same frequency, and compare the power output from this system to the power from only one row. We hope to see the power in-

crease as the number of rows when the array is operating at a single frequency.

Our ultimate goal in this project is detection of the envelope or pulse. Although we expect approximately 5 GHz for a pulse repetition rate in the time domain, this signal is to be carried by a wave at approximately 120 GHz. In order to detect the low-frequency pulses, we will also need to mix the signal down using Josephson technology.

References

- [1] Yukon, S.P., N.C.H. Lin, *Macroscopic Quantum Phenomena and Coherence in Superconducting Networks*, Singapore, p.351 (1995).
- [2] Yukon, S.P., N.C.H. Lin, *IEEE Trans. Appl. Sup.* 5 2959 (1995).
- [3] Duwel, A.E., P. Caputo, A.V. Ustinov, T.P. Orlando, unpublished work.
- [4] HYPRES, Inc., Elmsford, NY 10523.